

Particle incorporation by melt stirring for the production of metal-matrix composites

G. S. HANUMANTH, G. A. IRONS

Department of Materials Science and Engineering, McMaster University, 1280 Main Street West, Hamilton, Ontario, Canada L8S 4L7

The production of ceramic particle-reinforced metal-matrix composites by the melt-stirring technique involves two different steps: firstly, the establishment of particle–melt contact, and secondly, the wetting of the particles by the melt. The wetting behaviour of metal–ceramic systems has been studied extensively, whereas the contacting problem has been largely neglected. In this paper, a novel *in situ* thermal method has been used to investigate the kinetics of particle–melt contacting, based on melt cooling during and immediately after the particle addition. An enthalpy balance relates the amount of cooling and the fraction of the particles contacting the melt. For the aluminium alloy (A356) with 15 vol% silicon carbide (17 μm diameter), it was found that only 16% of the particles contacted the melt after mixing times of 15 min, but contact could be improved to 36% by adding magnesium to the melt. The fraction contacting the melt agreed well with the particle volume fraction calculated independently. Sampling of the froth layer on top of the melt revealed that a large portion of the particles resides there prior to incorporation into the melt.

Nomenclature

C_p	Specific heat ($\text{J kg}^{-1} \text{K}^{-1}$)
f	Fraction of added particles in contact with the melt
m	Mass (kg)
Q	Net rate of heating of the melt from electrical Power (W)
t	Time (s)
T	Temperature ($^{\circ}\text{C}$)
ϕ	Volume fraction
ρ	Density (kg m^{-3})
Θ	Contact angle (deg)

Subscripts

c	Composite
g	Gas
i	Initial
L	Liquid
m	Mixing
p	Particle
r	Recovery
s	Starting

1. Introduction

Metal-matrix composites (MMCs) are a relatively new class of engineering materials in which a strong ceramic reinforcement is incorporated into a metal matrix to improve its properties. The most commonly used reinforcements are SiC and Al_2O_3 fibres and particles, and the addition of these reinforcements to aluminium alloys has been the subject of a considerable amount of research work [1]. The majority

of the research efforts have focused on the mechanical properties of such materials, but there has been comparatively little research on the fundamental aspects of MMC processing.

An economical processing route to make MMCs, for applications where only moderate improvements in properties over the unreinforced alloy are required, involves the stirring of ceramic particles into melts. A technology based on this method to produce aluminium alloy MMCs has been commercialized by Alcan. Two major problems with this method are: firstly, the particles are generally not wetted by the liquid metal, and secondly, the particles tend to sink or float depending on their density relative to the liquid. Some of the fundamental issues regarding particle sedimentation during liquid-metal processing of MMCs have been recently investigated by the authors [2, 3]. The purpose of the present work was to examine the wettability problem during the incorporation of SiC particles into aluminium alloys by the melt-stirring process.

There has already been a considerable amount of work carried out on wettability measurements relevant to MMC systems. The contact angle, Θ , has been measured with sessile drops of liquid metal on a substrate of the reinforcement material in a well-controlled atmosphere at constant temperature [4]. In the aluminium–silicon carbide system, it has been found that the contact angle changes over time, and this finding has been attributed to chemical reactions occurring at the metal–substrate interface, such as formation of Al_4C_3 layer, and dissolution of SiC into aluminium. In other related studies, attempts were

made to lower the contact angle and improve wettability, by adding wetting agents such as magnesium, or by applying a suitable metallic coating, such as copper, silver or nickel, on the ceramic reinforcement. Magnesium has been found to reduce the surface tension of aluminium, and thereby the contact angle, as required by the Young–Dupre equation [5, 6]. This result was subsequently utilized by several authors to improve the wetting property in relation to the synthesis of MMCs [6–8]. Metallic coatings on ceramic reinforcements were found to be effective in improving wettability significantly [6]. The drawback is that, apart from the increased cost, these coatings render the reinforcement susceptible to chemical attack by the liquid metal, leading to the formation of undesirable intermetallic compounds. For instance, in the aluminium–ceramic system, nickel coatings applied to the ceramic reinforcement result in the formation of the intermetallic compound, NiAl_3 , which embrittles the matrix, and consequently degrades the mechanical properties of the composite [9].

The sessile drop contact angle is a useful measure of the thermodynamic potential for the wetting of metal by a ceramic phase. However, in practice, the incorporation of the ceramic phase into metals has to be carried out under conditions vastly different from those existing in the sessile drop experiment. For example, the molten metal or the particle or both may be covered by an oxide layer which hinders metal–particle contact, and gas may be entrained by the mixing process which could further delay the wetting process. Further, in commercial MMC processing the ceramic–metal contact is characteristically dynamic, whereas the sessile drop experiment is carried out under static conditions. All the above differences call for caution when using sessile drop contact angles to assess wettability in practical situations.

The present study was motivated by the need to understand the kinetics of the mixing and wetting processes under conditions that typically prevail during the commercial production of MMCs. As a first step towards this goal, experimental techniques have been developed to investigate the kinetics of the mixing and wetting processes in the manufacture of SiC particulate-reinforced aluminium-alloy metal composites.

2. Experimental procedure

2.1. Equipment

Mixing of silicon carbide particles with the molten aluminium alloy was carried out in a clay graphite crucible with an inside diameter of 0.3 m, placed inside a 10 kW resistance-heated furnace (see Fig. 1). The top of the crucible was covered with a Fibrefrax® insulation board with a port in the centre for particle addition, and insertion of the mixer and sampling devices. The particles were mixed into the melt using a pitched-blade turbine impeller with a diameter of 0.1 m. The impeller was fabricated from graphite, and driven by a variable speed a.c. motor. The impeller shaft was made of a 12 mm diameter mild steel rod, and enclosed in a graphite sleeve to prevent contact

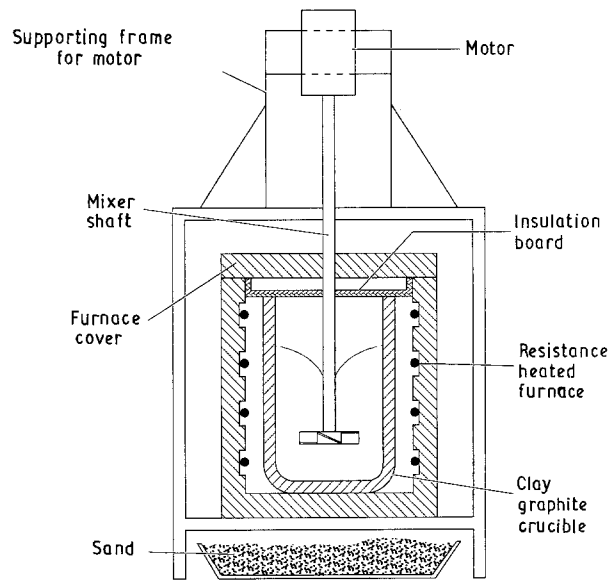


Figure 1 Schematic diagram of the experimental apparatus.

with the molten aluminium. All joints were sealed with the high-temperature ceramic adhesive, Ceramabond 552 (Aremco Products, Inc., New York).

For obtaining samples of the froth that accumulated on the melt surface, a specially designed froth sampler was used. It consisted of two split halves of a mild steel pipe, ~20 mm diameter, that could be opened and closed by a hinge mechanism. When the pipe was closed, a disc attached to one segment of the pipe automatically closed the bottom of the pipe. A mild steel rod was fixed concentrically within the pipe in order to serve as a heat sink for the solidifying metal. When the froth sampler was immersed in the crucible and closed, a portion of the froth solidified in the annular space between the mild steel rod and the walls of the pipe. Further, to allow easy removal of the solidified froth, the walls of the pipe were coated with graphite powder. This was accomplished by applying several layers of slurried graphite powder to the walls, and subsequent drying at high temperature.

2.2. Materials

The metal matrix used in this study was a commercial foundry alloy A356 (Alcan Int. Ltd, Canada) which is often used for metal-matrix composites. The major alloying elements in this alloy are 7.3% Si and 0.33% Mg. The high silicon content is reported to inhibit the formation of the brittle phase Al_4C_3 at the metal–SiC interface [10].

The green silicon carbide particles used in the experiments were supplied by Norton Advanced Ceramics, Canada. The size distribution of the particles was measured with a Horiba CAPA-700 Particle Analyser (Horiba Ltd, Japan). The particles had a median size of 17 μm , with a standard deviation of 8 μm .

2.3. Procedure

Initially, about 26 kg A356 alloy was charged into the crucible, and heated to about 640 °C which is well

above the liquidus temperature of 613 °C. Then, the impeller was lowered into the melt and attached to the motor, the clearance between the impeller and the bottom of the crucible being about 50 mm. The mixer was turned on and set to the predetermined speed. If an additional dose of the wetting agent, magnesium, was desired, it was added to the melt in the form of metal turnings. A J-type (iron-constantan) thermocouple was inserted into the melt to measure its temperature. The thermocouple was interfaced to a micro-computer to record the temperatures. Before temperature recording started, the heat input from the furnace to the crucible was set to the maximum level which marked the beginning of the melt-heating phase of the experiment. Following this, the melt temperatures were recorded at intervals of 30 s. The melt heating rate was used to determine the net amount of heat actually received by the melt from the heating elements. When the melt temperature rose to the predetermined initial value T_i , which was always between 690 and 700 °C, particle addition was started. Particles were added manually at a uniform rate over a time period of approximately 13 min, the total quantity of particles amounting to a nominal volume fraction of 0.15 (equivalent to 5.9 kg). Immediately after the completion of particle addition, the mixer was briefly turned off while a pin sample of the molten composite was withdrawn by suction into an 8 mm diameter Pyrex tube from near the centre of the melt. The sample solidified rapidly as it was being removed from the crucible. Following this, a sample of the froth resting on the melt surface was withdrawn using the froth sampler.

The mixing was continued for a duration of 180 min, with the sampling procedure being repeated at 30, 60, 120 and 180 min. Once the temperature recovered to the initial value T_i it was held constant for the remainder of the experiment. The samples were prepared for analyses in the following manner: the pin sample was removed from its glass shell, and any glass still adhering to the sample was removed by grinding. A 20–30 mm long section was cut and cleaned. This contaminant-free sample section was used in the subsequent analyses.

The density of the sample, ρ_c , was measured by using a standard specific gravity bottle. Following this, the carbon concentration, in weight per cent, of the sample was determined by combustion in a Leco volumetric carbon analyser (Leco Corporation, MI, USA). From the carbon concentration of the sample and the stoichiometry of silicon carbide, the volume fraction of SiC, ϕ_p , was calculated using the expression

$$\phi_p = \left(\frac{\text{wt\% carbon}}{100} \right) \left(\frac{\text{at wt SiC}}{\text{at wt C}} \right) \left(\frac{\rho_c}{\rho_p} \right) \quad (1)$$

Then, knowing the SiC volume fraction, ϕ_p , and the densities of the sample, ρ_c , the alloy A356, ρ_L , and SiC, ρ_p , the porosity, ϕ_g , was calculated by solving simultaneously the equations

$$\phi_L \rho_L + \phi_g \rho_g + \phi_p \rho_p = \rho_c \quad (2)$$

$$\phi_L + \phi_g + \phi_p = 1.0 \quad (3)$$

3. Results

Fig. 2 shows the thermal history of the melt before and after particle addition during an experiment. Maximum furnace power was applied and maintained throughout the experiment, so the section from 0 to t_s yields the effective heating rate of the melt, Q , according to

$$Q = m_L C_{pL} \frac{dT}{dt} \quad (4)$$

where dT/dt is the slope of the heating segment of the curve. Once particle addition starts at time t_s , the melt temperature begins to fall steadily from its initial temperature T_i , and only starts to rise after all the particles are added. The time at which the melt and particles regain the initial temperature, T_i , is t_r . Under these circumstances, the melt enthalpy is unchanged because the melt is restored to its initial temperature. Consequently, all the heat delivered by the furnace in the time interval $(t_r - t_s)$ seconds must be utilized to raise the particle temperature to T_i . The resulting increase in particle enthalpy is given by the expression

$$f m_p C_{pP} (T_i - T_0) = Q(t_r - t_s) \quad (5)$$

If the system were acting as a calorimeter, all the particles would be heated to the liquid temperature, and the time for temperature recovery could be easily calculated (by setting f equal to 1, and solving for t_r). However, the observed times are considerably shorter than expected, thus, a fraction f is introduced to account for the fact that only a fraction of the heat required to raise the temperature of all the particles to T_i is actually absorbed by the particles. This fraction f is a fraction of the particles added to the melt: 15 vol% of the melt in the present experiments. This implies that only a fraction of the added particles attain the melt temperature in times of the order of 1000 s. The SiC particles are so fine that once they contact the melt, they will be heated in the order of a

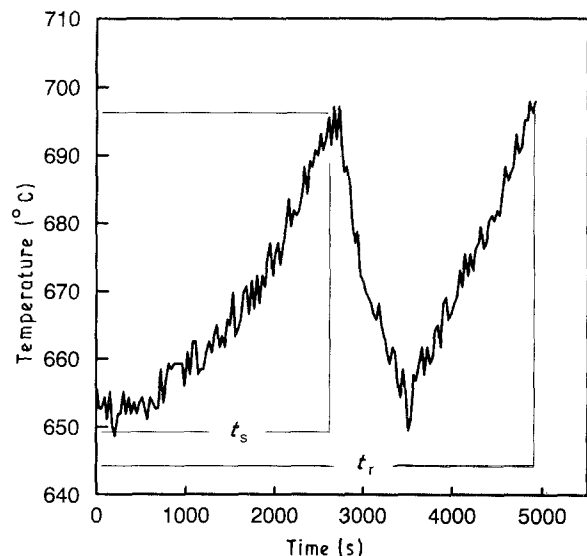


Figure 2 Typical temperature response of the melt showing the initial heating period of the melt, cooling due to particle addition, and the period of temperature recovery following the completion of particle addition.

microsecond [11], thus it is clear that the remaining fraction has neither contacted, nor been wetted by the melt.

Experiments were performed with different magnesium contents in the melt at a fixed impeller speed of 650 r.p.m. The fraction of the added particles in contact with the melt is plotted as a function of magnesium content in Fig. 3. It is quite striking that only 16% of the added particles contact the melt with no extra magnesium in the melt. Little improvement is seen in particle-melt contact until the magnesium content of the melt rises to 1 wt%, thereafter the amount of particles contacting the melt increases to 36% added particles.

The effect of impeller speed on the particle-melt contact was investigated at a fixed magnesium content of 1.5 wt%. The results are shown in Fig. 4 for an impeller speed range of 450–700 r.p.m. Interestingly, a more or less linear improvement of contact with impeller speed is observed up to a speed of about

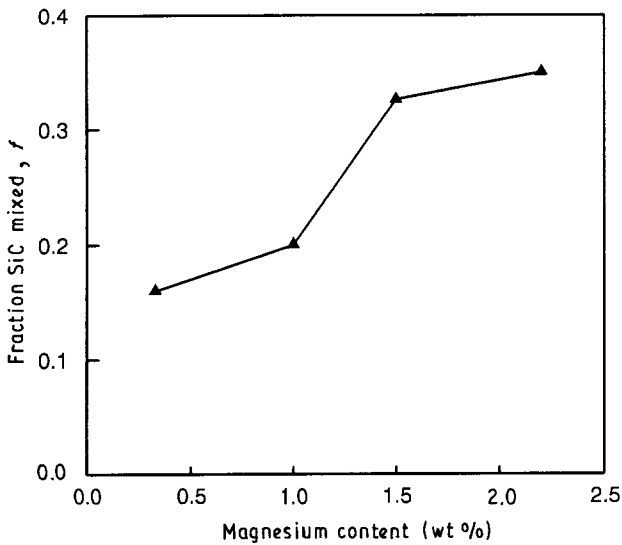


Figure 3 Fraction of the particles added to the melt, amounting to 15 vol %, which contacted the melt as a function of the magnesium content of the melt.

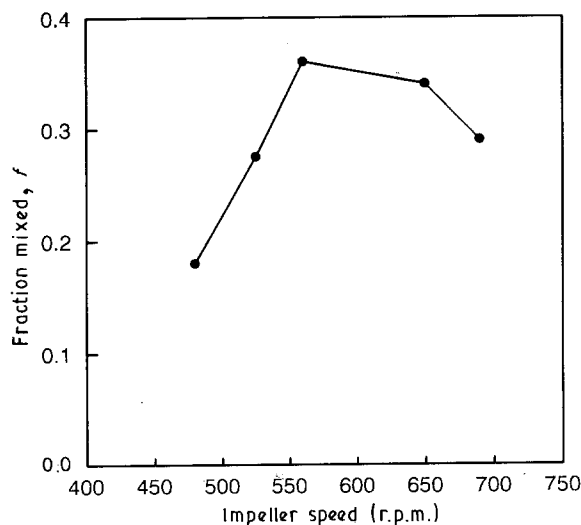


Figure 4 The effect of impeller speed on the fraction of the 15 vol % particles added to the melt which contacted the melt, with 1.5 wt % Mg in the melt.

550 r.p.m., and above which, the contact decreases in a non-linear fashion.

Using the specific gravity and carbon concentration measurement techniques, the volume fraction of SiC, ϕ_p , and porosity ϕ_g , of the composite samples were calculated as a function of time of mixing, t_m . The results are presented in Figs 5 and 6, wherein ϕ_p and ϕ_g are plotted against time. Fig. 5 shows that there is good agreement between the fraction of particles contacting the melt obtained by the thermal method, and the actual fraction of particles mixed with the melt as measured by the chemical analysis method. The difference in mixing rates with and without added magnesium is more pronounced in the first 60 min mixing as depicted by the diverging curves. However, during the latter part of the mixing, the curves appear to be converging, suggesting that given enough time, the same degree of mixing could be achieved without adding an extra dose of magnesium.

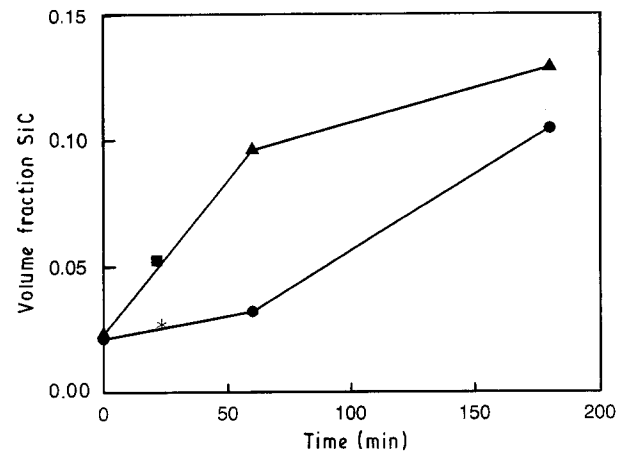


Figure 5 Particle volume fraction in the melt as a function of mixing time elapsed after the completion of particle addition, determined by melt sampling. There is good agreement with the particles in the melt inferred from the temperature information. Magnesium (wt %): (●) 0.33; (▲) 1.5; (■) 0.33, thermal method; (*) 1.5, thermal method.

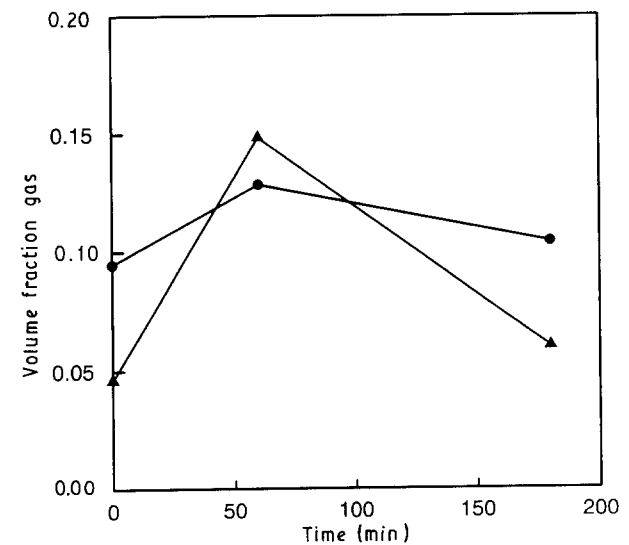


Figure 6 Porosity volume fraction in the melt as a function of mixing time elapsed after the completion of particle addition, determined by melt sampling. Magnesium (wt %): (●) 1.5, (▲) 0.33.

The porosity, ϕ_g , increases with time for both cases, although the values are slightly higher in the case of no added magnesium. After a peak value of about 0.15, ϕ_g decreases to more or less the starting value of about 0.05. Figs 7 and 8 illustrate the typical distribution of particles and porosity in a solidified pin sample withdrawn from the melt during the mixing process. A high degree of segregation of silicon carbide particles to the grain boundaries is evident in Fig. 7. In the microstructure of the pores shown in Fig. 8 it is noticed that the pores are usually bounded by a layer of closely spaced particles. Some of the porosity could be the result of the breakdown of silicon carbide particle agglomerates during the preparation of the sample for microscopic examination.

4. Discussion

The process of incorporation of particles in the melt appears to involve two steps.

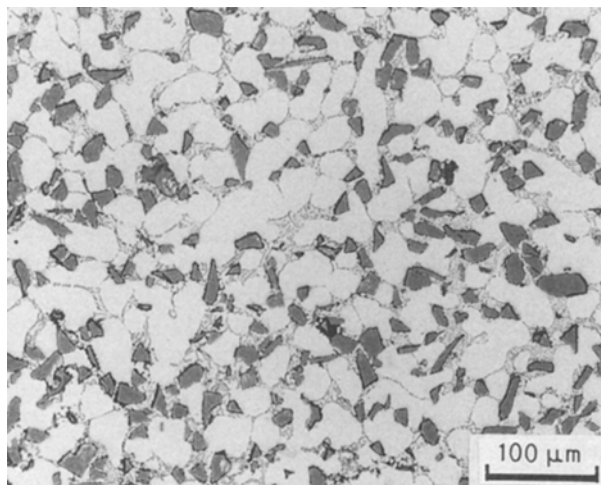


Figure 7 Microstructure showing the typical distribution of particles in an A356 composite containing 15 vol% silicon carbide particles.

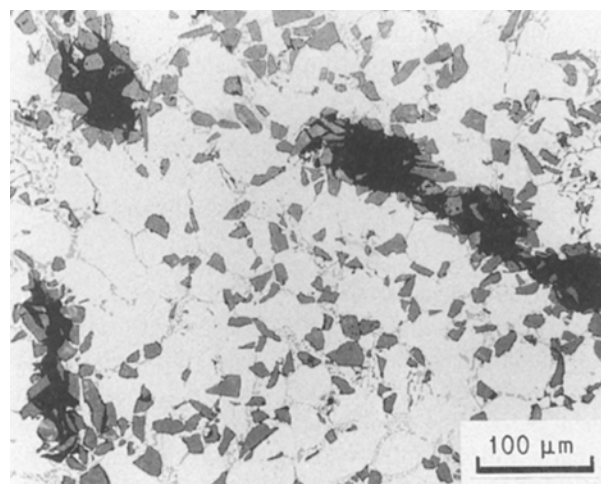


Figure 8 Microstructure showing the typical distribution of porosity and particles in an A356 composite containing 15 vol% silicon carbide particles.

1. The process of contacting the particle with the melt which can be monitored with the present techniques of melt temperature measurement and volume fraction measurement during mixing, and

2. The wetting of the particles by the melt which in the particular case of SiC/Al system is thought to involve the formation of aluminium carbide, and dissolution of silicon into aluminium [4].

Separating the incorporation process into two successive steps emphasizes the fact that particles in the melt are not necessarily wetted, and that contacting is a pre-requisite step for wetting.

Both of these steps are time dependent; Fig. 2 shows that it takes thousands of seconds for the particles to contact the melt, whereas previous studies with sessile drops of aluminium on silicon carbide substrate have shown that it takes hundreds of seconds for wetting to occur. Each particle will be at a different stage in these two steps depending on when it was added to the melt, and when it contacted the melt. Both of these steps are speeded by small contact angles, and low surface tension. Thus, the beneficial effects of magnesium observed in commercial practice may not be solely due to improved wettability, but may also be attributable to speedier contact of particles with the melt, as illustrated in Fig. 3. It is possible that the mixing/contacting step is a more serious rate limitation than the wetting step, simply based on the time required for each step, thousands of seconds compared to hundreds of seconds. Further work would be required to confirm this.

For the particles to contact the melt, the shear forces generated by the rotating impeller must overcome the interfacial forces that prevent the incorporation of particles. Two related problems complicate the incorporation process.

1. The particles tend to form agglomerates which must be broken up before complete dispersion and wetting can occur.

2. It is energetically conducive for the particles to become attached to gas bubbles, similar to froth flotation in mineral processing.

These problems are more acute in the froth layer, the depth of the froth being a measure of the amount of added particles rejected by the melt; the deeper the froth the higher the amount rejected. Initially, the froth layer is deep; measurement yielded values of about 130 mm. After 3 h mixing, the froth depth decreased to a final value of about 10–30 mm, reflecting the gradual incorporation of most of the particles. Further, the froth layer has a relatively high concentration of silicon carbide interspersed with large voids; typically $\phi_p = 0.16$ and $\phi_g = 0.18$. Some of the particles are in the form of large clusters, sectioning of the froth sample revealed pockets of SiC powder that evidently never contacted the melt. The macrostructure of the froth shown in Fig. 9 highlights these characteristics.

Fig. 4 shows that there is an optimal mixing speed of about 550 r.p.m. beyond which mixing efficiency drops. As mixing speed increases, so do shear stresses

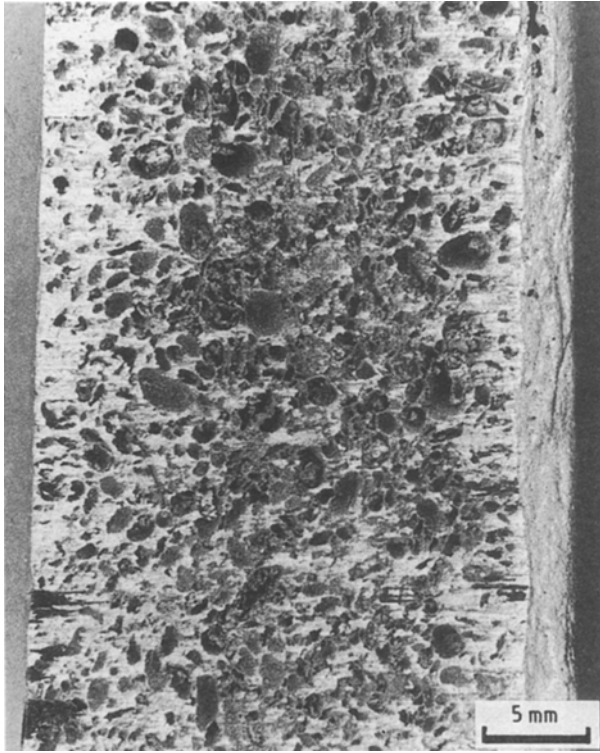


Figure 9 Macrostructure of the vertical section of a froth sample showing particle agglomerates and large pores.

in the melt. This is reflected in the increasing value of f . However, higher mixing speeds also result in increased gas entrainment by the melt, and increased bubble surface area for particle flotation. The competition between the opposite effects of increased shear stress and increased bubble surface area may result in the optimum mixing speed. At higher speeds, beyond the optimum speed of 550 r.p.m. there appears to be an increasing tendency for the particles to end up in the froth, giving rise to a fall in f value.

The porosity of the samples also follows a time-dependent function. Porosity arises from three causes: gas entrainment during mixing, hydrogen evolution and shrinkage on solidification. The method of sampling was designed to obtain rapid freezing of a small sample, thus the contribution to porosity from hydrogen evolution and shrinkage should remain unchanged from one sample to another. Therefore, variation in porosity is likely to result from a change in gas hold-up of the molten composite. The rate at which the molten composite can expel the entrained gas bubbles is expected to be strongly influenced by the melt viscosity. The addition of particles increases the viscosity [12] and results in a higher gas hold-up.

During particle addition, there is undoubtedly some local solidification of the melt induced by the particles; however, the time for melt-back is short [11] in comparison to the time for temperature recovery ($t_r - t_s$). Consequently, the method used to determine f is free from these effects. The fraction f determined by this technique is the fraction of added particles contacting the melt integrated over the time interval, and agrees well with the number determined by sampling the molten composite. It is rather ironic to note that if all the particles instantaneously contacted the melt,

the entire melt temperature would fall below the solidus (555 °C).

Because the contacting of the particles is slow, one may consider alternative methods to incorporate the particles. Pneumatic injection of the particles through a submerged lance is one possibility; however, the fraction of particles contacting the melt is only 0.3–0.5 for the injection of silica into lead [11]. Thus it appears that the high surface tension of liquid metals impedes good particle–liquid contact, in both pneumatic and stirring incorporation techniques.

The present technique to evaluate particle–liquid contact offers several advantages over other techniques:

1. the same materials used in commercial processes can be tested, whereas in sessile drop techniques a large substrate must be fabricated which may have different surface and structural characteristics;
2. this technique can be readily applied to commercial processes to evaluate the differences between various particles, melt chemistries, equipment configurations, and
3. the technique can be adapted to on-line process control and product-quality monitoring; for example, if the temperature response falls outside the normal range of acceptability, one must be suspicious of that material.

5. Conclusions

A novel technique was developed to assess the extent of particle–liquid contact during MMC processing. It is based on measurement of bath cooling during and immediately after particle addition. The contacting of 17 μm SiC particles with A356 aluminium alloy is surprisingly slow; only a fraction equal to 0.16 of the total amount of SiC particles (15 vol %) added to the melt actually contacted the melt in a timescale of the order of 1000 s. The fraction of particles contacting the melt agreed reasonably well with the result of an independent method developed to determine the particle volume fraction of melt samples. The fraction contacting the melt could be improved by:

1. addition of magnesium to the melt which reduces surface tension, and
2. using the optimum impeller speed of 550 r.p.m. for the present apparatus.

Sampling of the froth layer on top of the melt indicated that significant fractions of the particles were held up there prior to contact with the melt.

Acknowledgements

The authors thank Mr O. Kelly for help with the experimental work. The financial support of the Ontario Centre for Materials Research, the Natural Sciences and Engineering Research Council of Canada and an industrial consortium of Alcan, Inco, Ontario Hydro, Pratt and Whitney and Sherritt Gordon and the material donations from Alcan Int. Ltd and Norton Advanced Ceramics of Canada, are gratefully acknowledged.

References

1. H. MOSTAGHACI (ed.), "Processing of Ceramic and Metal Matrix Composites", Proceedings of the CIM conference of Metallurgists, Halifax, Nova Scotia (Pergamon Press, New York, 1989).
2. LAFRENIERE, S. and G. A. IRONS, in "International Symposium on Production, Refining, Fabrication and Recycling of Light Metals", Hamilton, ON (CIM, 1990) p. 177.
3. G. S. HANUMANTH, G. A. IRONS and S. LAFRENIERE, *Metall. Trans.*, **23B** (in press).
4. V. LAURENT, D. CHATAIN and N. EUSTATHOPOULOS, *J. Mater. Sci.* **22** (1987) 244.
5. F. DELANNAY, L. FROYEN and A. DERUYTTERE, *ibid.* **22** (1987) 1.
6. P. K. ROHATGI, R. ASTHANA and S. DAS, *Int. Metals Rev.* **31** (1986) 115.
7. F. A. GIROT, L. ALBINGRE, J. M. QUENISSET and R. NASLAIN, *J. Metals* November **39** (1987) 18.
8. A. MORTENSEN, J. A. CORNIE and M. C. FLEMINGS, *ibid.* February **40** (1988) 12.
9. S. SCHAMM, R. FEDOU, J. P. ROCHER, J. M. QUENISSET and R. NASLAIN, *Met. Trans.* **22A** (1991) 2133.
10. D. J. LLOYD, *Comp. Sci. Tech.* **35** (1989) 159.
11. G. A. IRONS and L. R. FARIAS, *Can. Metall. Q.* **25** (1986) 297.
12. M. MADA and F. AJERSCH, in "Metal and Ceramic Matrix Composites: Processing, Modelling and Mechanical Behaviour", edited by R. B. Bhagat, A. H. Clauer, P. Kumar and A. M. Ritter (The Minerals, Metals and Materials Society, Warrendale, Pa, 1990) p. 337.

*Received 27 April
and accepted 29 October 1992*